European Journal of Mechanics B/Fluids 64 (2017) 2–7

Contents lists available at ScienceDirect

European Journal of Mechanics B/Fluids

journal homepage: www.elsevier.com/locate/ejmflu

Validity range of linear kinetic modeling in rarefied pressure driven single gas flows through circular capillaries

Dimitris Valougeorgis [a,*], Nikos Vasileiadis [a], Vladimir Titarev [b]

[a] Laboratory of Transport Phenomena, Department of Mechanical Engineering, University of Thessaly, Pedion Areos, 38334 Volos, Greece

[b] Federal Research Center "Computer Science and Control" of RAS, Moscow 119333, Russia

HIGHLIGHTS

- The range of validity of linear kinetic modeling in simulating rarefied gas flows in capillaries is computationally investigated.
- The applicability margins are specified in terms of the gas rarefaction, pressure ratio and tube aspect ratio.
- It is deduced that linear solutions are valid in a much wider range than expected resulting in great computational savings.
- Specific applicability criteria are provided.

ARTICLE INFO

Article history:
Available online 4 November 2016

Keywords:
Kinetic theory
Kinetic modeling
Rarefied capillary flows
DSMC

ABSTRACT

The range of validity of various linear kinetic modeling approaches simulating rarefied pressure driven gas flow through circular tubes is computationally investigated by comparing the flowrates obtained by the linear approaches with the corresponding nonlinear ones. The applicability margins of the linear theories in terms of the parameters determining the flow (gas rarefaction, pressure ratio, tube aspect ratio) are specified, provided that the introduced deviation norm is smaller than a specific value. The work is motivated by the fact that computational effort is significantly reduced when linear, instead of nonlinear, kinetic modeling is implemented. It is found that the range of validity of the linear solutions is much wider than the expected one, as defined by their formal mathematical constrains and it remains valid in a range of parameters, where the DSMC method and nonlinear kinetic modeling become computationally inefficient, resulting in great computational savings.

1. Introduction

Rarefied single gas flows through circular tubes of finite length driven by various pressure differences have attracted, over the years, considerable attention due to their wide applicability in industrial processes and technological applications operating in the whole range of the Knudsen number [1–13]. In most cases, the flow problem is numerically solved either stochastically based on the direct simulation Monte Carlo (DSMC) method [14] or deterministically based on the direct numerical solution of the Boltzmann equation (BE) [15] as well as of suitable kinetic model equations [1,2,6]. Very good agreement between corresponding results obtained by the DSMC method, the BE and kinetic models (BGK [16], ES [17], Shakhov [18]) has been observed for flows through orifices and tubes of finite length subject to various ratios of the downstream over the upstream pressure including expansion into vacuum [8,19,20]. This good comparison is sustainable across all flow regimes. In addition, computational results match experimental data very well [5,21–23].

In spite the simple geometry of the flow configuration, the required computational effort (CPU time and memory) to simulate pressure driven rarefied gas flows through tubes of finite length, is considerable. This is due to the number of involved parameters specifying the flow and the size of the computational domain [3–6]. The dimensionless parameters fully determining the flow setup are the reference Knudsen number (or rarefaction parameter), the ratio of the downstream over the upstream pressure and the tube aspect ratio (length over radius). The computational domain includes the tube as well as large upstream and downstream regions (reservoirs) in order to properly impose boundary conditions for the incoming distributions at kinetic level.

The computational effort may be significantly reduced when linear (instead of nonlinear) kinetic modeling is introduced based

* Corresponding author.
E-mail address: diva@mie.uth.gr (D. Valougeorgis).

http://dx.doi.org/10.1016/j.euromechflu.2016.11.004
0997-7546/

on the linearized version of kinetic model equations. In linear modeling the number of parameters is reduced and in some cases the upstream and downstream regions are eliminated. Of course, linear treatment itself is subject to several restrictions such as very small pressure differences and very large capillary aspect ratios. As noted in [24], the validity of linear theory is ensured for flows in the free molecular and lower part of the transition regimes by small Mach numbers and for flows in the upper part of the transition and slip regimes by small Reynolds numbers. It has been recently shown however, that the various implemented linear kinetic approaches may capture the correct behavior of the flow field well beyond their formal mathematical limitations [25–29]. Taking into consideration that the DSMC method and nonlinear kinetic modeling become computationally inefficient exactly in the range of parameters where linear treatment may still be valid it is of practical interest to investigate in a detail and systematic manner the range of applicability of the various linear kinetic theories. There is also theoretical interest, since the numerical solvers of the governing linearized kinetic equations are amenable to mathematical treatment.

The aim of the present work is to computationally investigate the range of validity of the various linear kinetic modeling approaches and to provide their specific applicability margins within some accepted deviation in terms of the involved parameters determining the flow conditions. The decision is made by comparing the flowrates obtained by linear approaches with corresponding nonlinear ones, based on available data from previous works [4,5,10,13,26–28], as well as on additional results obtained in the present work in order to cover an adequately wide range of all involved parameters. Such an analysis comparing linear and nonlinear results has been made for slit flow in [25,29] and for orifice flow in [29].

2. Flow configuration and modeling

Although the flow configuration is well known [4–6], it is also described here for completeness and clarity. Consider the steady-state monatomic gas flow through a tube of length L and radius R, connecting two vessels denoted by A and B. The gas pressures P_A, P_B and temperatures T_A, T_B at the two vessels, far from the connecting tube, are maintained constant with $P_A > P_B$ and $T_A = T_B$. The walls of the reservoirs and of the tube are also maintained at temperature T_A. The flow setup with the coordinate system and its origin are shown in Fig. 1. Due to the pressure difference there is an axisymmetric flow in the axial direction with the macroscopic distributions varying in the radial and axial directions. At the open boundaries (dotted lines) the gas is at rest and the incoming distributions are the local Maxwellian ones. The volume of the upstream and downstream vessels is large enough to ensure proper implementation of the boundary conditions at the open boundaries. At the walls (solid lines) purely diffusive gas–surface interaction is considered. Along the symmetry axis $\hat{r} = 0$ purely specular reflection is applied. It is assumed that the flowing monatomic gas consists of hard-sphere molecules. The quantities at vessel A far from the tube are taken as the reference ones. Also, the reference length and velocity are the tube radius R and the most probable speed $\upsilon_A = \sqrt{2R_gT_A}$ respectively ($R_g = k_B/m$, with k_B being the Boltzmann constant and m the molecular mass, denotes the gas constant).

This flow configuration is five-dimensional (two dimensions in the physical space and three in the velocity space) and it is defined by three dimensionless input parameters: (i) the reference gas rarefaction parameter

$$\delta_A = \frac{P_A R}{\mu_A \upsilon_A} \tag{1}$$

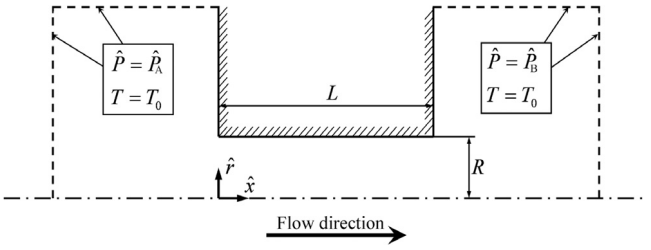

Fig. 1. View of the flow configuration.

with μ_A being a reference viscosity at temperature T_A, (ii) the pressure ratio P_B/P_A and (iii) the aspect ratio L/R.

The quantity of major practical importance is the mass flowrate defined as

$$\dot{M}_{NL} = 2\pi \int_0^R m\hat{n}\left(\hat{r}, \hat{z}\right) \hat{u}_z\left(\hat{r}, \hat{z}\right) \hat{r} d\hat{r}. \tag{2}$$

Introducing $r = \hat{r}/R$ as well as the dimensionless number density $n = \hat{n}/n_A$ and axial component of the bulk velocity $u_z = \hat{u}_z/\upsilon_A$, the mass flow rate is rewritten as

$$\dot{M}_{NL} = \frac{\sqrt{\pi} R^2 P_A}{\upsilon_A} W_{NL} \tag{3}$$

where

$$W_{NL} = 4\sqrt{\pi} \int_0^1 n\left(r, z\right) u_z\left(r, z\right) r dr \tag{4}$$

is the dimensionless flowrate. The subscript "*NL*" denotes nonlinear results. The dimensionless flow rate W_{NL} has been computed, based on the DSMC method, the Boltzmann equation and the nonlinear BGK and Shakhov kinetic model equations, in terms of $\delta_A \in \left[0, 10^2\right]$, $P_B/P_A \in [0, 0.9]$ and $L/R \in [0, 50]$ in [4,5,10,13,19].

For the needs of the present work the DSMC results for flow through tubes up to $L/R = 10$ into vacuum and various pressure ratios, reported in [4,5] respectively, have been introduced. The results in [10], based on the Shakhov model, have been implemented for flow through longer tubes with $10 \leq L/R \leq 50$ into vacuum. Furthermore, additional results based on the BGK and Shakhov models have been obtained here, within the aforementioned range of parameters, in order to have an adequately dense database of the nonlinear flowrates. In all cases modeling is based on hard sphere molecules with purely diffuse gas–surface interaction. As noted in [8,19,20], all approaches provide corresponding results in very good agreement and therefore using either the DSMC method or the BGK or the Shakhov models to build the flowrate database does not affect the concluding remarks concerning the applicability range of the linear schemes. The implemented DSMC solver is described in detail in [4,5]. The solution of the BGK and Shakhov models is obtained discretizing the physical space by a second order scheme and the molecular velocity space by the discrete velocity method. This deterministic approach has been described and successfully applied in several flow and heat transfer configurations [2,6,15,27,30,31]. The introduced numerical error (uncertainty) in the computed flow rates is always taken less than 1%. These nonlinear flowrates are used as the reference ones, in order to investigate the applicability of the linear approaches.

In general, the computational effort is increased as δ_A is increased and the gas flow becomes less rarefied as well as the tube aspect ratio L/R is increased. In the implemented DSMC algorithm the computational effort is also increased as the pressure ratio P_B/P_A approaches one, while on the contrary, the convergence speed of the deterministic discrete velocity codes remains approximately the same at any pressure ratio. In addition, the DSMC code runs in serial mode, while the deterministic codes

are highly parallelized. The involved computational effort depends on the set of flow parameters and on the code optimization and for the prescribed accuracy it may vary from few hours up to several days of CPU time.

3. Linearized methodologies with corresponding results and discussion

Depending upon the assumptions made, linearization may be performed in three ways. The first and more general one is based solely on the assumption of very small difference between the upstream and downstream pressures, i.e. $\Delta P/P_A \ll 1$ [26,28,29]. The other two are both based on the infinite capillary theory (i.e., fully developed flow in long channels with small local pressure gradients), without [1,30,31] and with end effect corrections [28,31–34].

In the discussion to follow the implementation of a linear approach will be considered as valid provided that the norm of the relative deviation between corresponding nonlinear and linear results is smaller than a specific value. In the present work this upper limit of the deviation norm is set to 10%, since for engineering purposes this deviation is considered in most cases as accepted. Based on the presented results similar decisions on the validity of the linearized theories may be taken for smaller or larger accepted deviations.

In the first linearization approach the flow configuration is as shown in Fig. 1, i.e. both inlet and outlet regions are included in the computational domain. However, the solution now depends only on δ_A and L/R, while due to linearization, it is independent of P_B/P_A, resulting to significant savings in computational resources. This linearized flow configuration has been recently solved in [26,27] based on the linearized Shakhov and BGK models respectively. The linearized mass flowrate, neglecting second order terms in $\Delta P/P_0$, is given by

$$\dot{M}_{LIN} = \frac{\sqrt{\pi} R^2 \Delta P}{\upsilon_0} W_{LIN} \tag{5}$$

where

$$W_{LIN} = 4\sqrt{\pi} \int_0^1 u_z\,(r, z)\, r dr \tag{6}$$

is the dimensionless linearized flowrate reported in [26,27]. The subscript "*LIN*" denotes linear results. It is readily seen that the ratio of the linearized over the nonlinear mass flowrates is given by

$$\frac{\dot{M}_{LIN}}{\dot{M}_{NL}} = \left(1 - \frac{P_B}{P_A}\right) \frac{W_{LIN}}{W_{NL}} \tag{7}$$

with W_{LIN} being a function only of δ_A and L/R, while W_{NL} being a function of all three parameters. In the present work, W_{LIN} is based on the linearized BGK results presented in [27].

In Fig. 2, the relative percentage deviation

$$\varepsilon_{LIN} = \left[\left(\dot{M}_{NL} - \dot{M}_{LIN}\right)/\dot{M}_{NL}\right] \times 100 \tag{8}$$

is plotted for flow through a tube in terms of $\delta_A \in \left[10^{-2}, 20\right]$ for $P_B/P_A = [0.9, 0.5, 0.1, 0]$ and $L/R = [5, 10, 20]$. The positive and negative values of the deviation indicate that the linear mass flowrates are smaller and larger of the corresponding nonlinear ones respectively. A detailed view of the introduced deviation in terms of the involved parameters is provided. The deviation is within the accepted range of $\pm 10\%$ for all pressure ratios when $L/R = 20$ and then, for $L/R = 10$ and $L/R = 5$ only when $P_B/P_A \geq 0.1$ and $P_B/P_A \geq 0.5$ respectively. It is obvious that as L/R is decreased, the pressure difference must be reduced in order to sustain the validity of the linear analysis. For $\delta_A < 10^{-2}$ the deviation remains, in all cases, within $\pm 10\%$, while is rapidly increased for $\delta_A > 10$. This is a clear indication that linear analysis may be applied to small but finite pressure differences ($P_B/P_A = 0.9$), as well as to moderate ($P_B/P_A = 0.5$) and even large ($P_B/P_A = 0.1$)

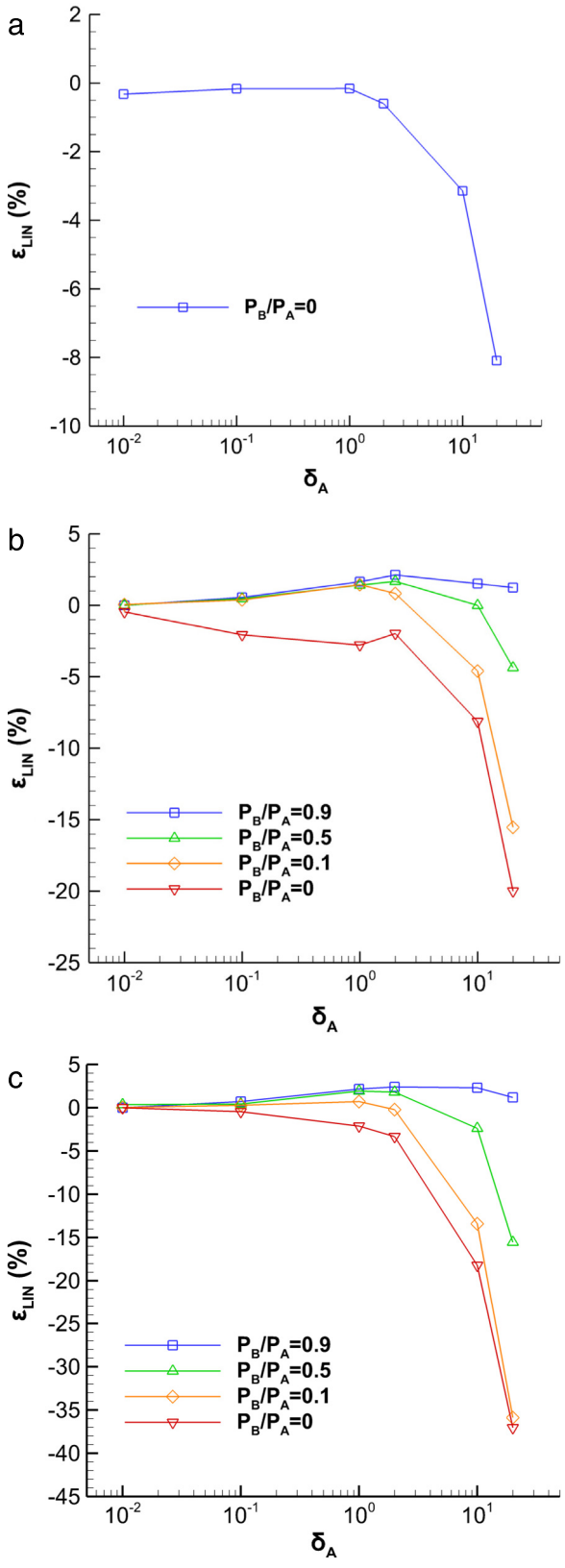

Fig. 2. Relative percentage deviation ε_{LIN} of the linear solution compared to the nonlinear one in terms of δ_A and various P_B/P_A for flow through tubes of (a) $L/R = 20$, (b) $L/R = 10$ and (c) $L/R = 5$.

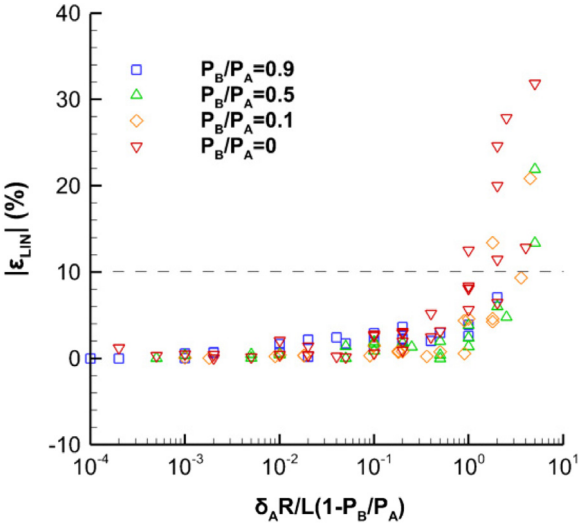

Fig. 3. Norm of the relative percentage deviation $|\varepsilon_{LIN}|$ of the linear solution compared to the nonlinear one for flow through a tube in terms of $\delta_A\,(R/L)\,(1-P_B/P_A)$.

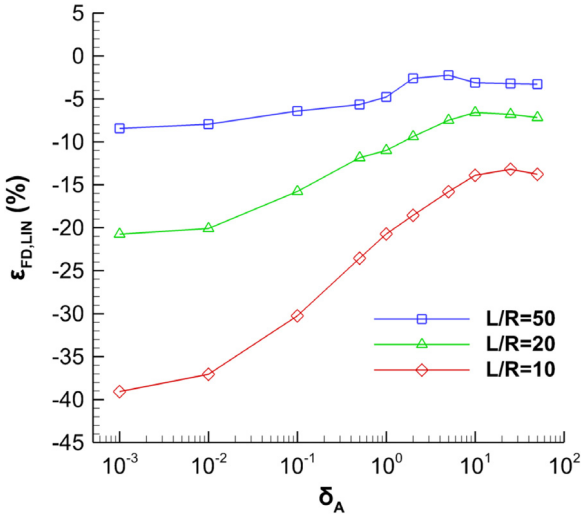

Fig. 4. Relative percentage deviation $\varepsilon_{FD,LIN}$ of the fully developed solution without end effect correction compared to the linear one in terms of δ_A for flow through a tube of various L/R.

pressure differences depending upon the specific values of L/R and δ_A. The present observations for flow through a tube are compatible with the ones made in [29] for orifice flow ($L/R = 0$), i.e. that the range of applicability of linear theory in terms of δ_A becomes larger as the pressure difference is decreased, as well as that linear and nonlinear results may be very close even at moderate pressure ratios (e.g. $P_B/P_A = 0.7$ or 0.5) provided that the gas flow is adequately rarefied.

A more compact picture of the deviation dependency on all parameters is provided in Fig. 3, where the norm of the relative deviation $|\varepsilon_{LIN}|$ is plotted in terms of the quantity $\delta_A\,(L/R)\,(1-P_B/P_A)$. It is seen that $|\varepsilon_{LIN}| \leq 10\%$ provided that

$$\delta_A \left(\frac{R}{L}\right)\left(1-\frac{P_B}{P_A}\right) \leq 1. \tag{9}$$

Inequality (9) is the condition which must be satisfied, independently of the specific values of each of the three parameters, in order to apply linearization provided that an introduced maximum deviation within $\pm 10\%$ is permissible. In the case where the permissible error is only $\pm 1\%$ the condition to be fulfilled becomes

$$\delta_A \left(\frac{R}{L}\right)\left(1-\frac{P_B}{P_A}\right) \leq 0.005. \tag{10}$$

Next, the limitations of the infinite capillary theories are examined starting with the one without end effect correction, which is by far the most simple and widely used linear treatment [1,32]. Assuming $L/R \gg 1$, the flow is considered as fully developed and end effects at the inlet and outlet of the tube are ignored. In addition, pressure (and density) varies only in the flow direction and remains constant at each cross section of the channel, i.e. $P = P\left(\hat{z}\right) \in [P_A, P_B]$, with $\hat{z} \in [0, L]$. The flow is driven by the imposed pressure difference $\Delta P = P_A - P_B$ between the inlet and outlet of the tube. Following a well-known procedure it is readily deduced that the mass flow rate, as defined by Eq. (2), may be rewritten in the case of fully developed flow as [1,32]

$$\dot{M}_{FD} = \frac{\pi R^3}{\upsilon_A}\frac{\Delta P}{L} W_{FD}. \tag{11}$$

In Eq. (10),

$$W_{FD} = \frac{1}{\delta_B - \delta_A}\int_{\delta_A}^{\delta_B} G_{FD}\, d\delta \tag{12}$$

is computed by integrating the reduced flow rate $G_{FD}\,(\delta)$ between the inlet and outlet rarefaction parameters δ_A and δ_B respectively, accordingly defined by the corresponding pressures P_A and P_B. The subscript "FD" denotes fully developed results. Since $G_{FD}\,(\delta)$ depends only on δ and no inlet and outlet regions are considered the computational effort required in the implementation of the infinite capillary theory is negligible. Extensive results of $G_{FD}\,(\delta)$ may be easily found in the literature [1,32,37,38]. Here, the values of the reduced flow rate $G_{FD}\,(\delta)$ are based on the linearized BGK model [1,32,38]. The ratio of the fully developed mass flowrate over the corresponding linear one is given by

$$\frac{\dot{M}_{FD}}{\dot{M}_{LIN}} = \sqrt{\pi}\frac{R}{L}\frac{W_{FD}}{W_{LIN}}. \tag{13}$$

The relative percentage deviation

$$\varepsilon_{FD,LIN} = \left[\left(\dot{M}_{LIN} - \dot{M}_{FD}\right)/\dot{M}_{LIN}\right] \times 100 \tag{14}$$

of the fully developed solution (without end effect correction) compared to the linear one in terms of $\delta_A \in \left[10^{-3}, 50\right]$ for various L/R is plotted in Fig. 4. In all cases the deviation is negative implying that the fully developed approach overestimates the computed flow rates. As L/R is increased the deviation is significantly reduced, always having in terms of δ_A a nonmonotonic behavior with a shallow minimum in the transition regime. In the slip regime $\varepsilon_{FD,LIN}$ is slightly increased, while in the free molecular regime is significantly increased. This is due to the flow developing length in the tube, which is increased as the flow becomes more rarefied and therefore, for $L/R = 10$ and 20 the tube is not long enough to assume fully developed flow for $\delta_A < 1$. On the contrary for $L/R = 50$ the deviation of the fully developed solution compared to the linear one remains small in a wide range of gas rarefaction. Overall, the infinite capillary theory without end effect correction will result to a deviation within $\pm 10\%$ provided that inequality (9) is fulfilled and $L/R \geq 50$. The fact that in order to justify the fully developed assumption, the condition $L/R \gg 1$ must be accompanied by a supplementary restriction in the form of inequality (9), when the flow is not adequately rarefied, has been previously pointed out in [32,39].

The more advanced implementation of the infinite capillary theory is the one with the inclusion of the end effect correction [1,28,33–36]. The main idea of the end effect theory is to correct the real capillary length L/R by additional lengths $\Delta L_1/R$ and

Table 1
Length increment $\Delta L/R$ for various values of the rarefaction parameter δ_A [26].

δ_A	0.005	0.05	0.1	0.2	0.4	0.6	0.8	1	2
$\Delta L/R$	2.22	1.72	1.52	1.33	1.16	1.07	1.01	0.964	0.841
δ_A	4	6	8	10	…	∞			
$\Delta L/R$	0.735	0.704	0.688	0.682	…	0.680			

Table 2
Relative percentage deviation $\varepsilon_{EE,LIN} = \left[\left(\dot{M}_{LIN} - \dot{M}_{EE}\right)/\dot{M}_{LIN}\right] \times 100$ of the end effect solution compared to the linear one for flow through a tube for various L/R and δ_A.

L/R	δ_A						
	0.01	0.1	1	2	10	25	50
1	25.16	11.06	−0.30	−0.87	−2.00	1.32	−8.63
2	17.93	6.37	−1.05	−1.16	−1.36	1.03	−5.83
5	8.32	1.56	−1.38	−1.22	−0.86	0.68	−2.75
10	3.35	0.11	−1.21	−1.49	−0.73	0.38	−0.15
20	0.68	−0.51	−1.24	−0.92	−0.29	−0.01	−0.34
50	1.39	−0.32	−0.90	0.72	−0.38	−0.49	−0.55

$\Delta L_2/R$ taking into account the end effect phenomena at the inlet and outlet of the tube respectively. All other assumptions and characteristics of the fully developed flow, as described above, remain the same. Recently, based on the linearized BGK model a methodology has been introduced computing the corrective length $\Delta L/R$ only in terms of the reference rarefaction parameter δ_A independent of the tube length L/R [28]. Following the end effect correction theory the mass flowrate is given by

$$\dot{M}_{EE} = \frac{\pi R^3}{\upsilon_A}\frac{\Delta P}{L} W_{EE} \tag{15}$$

where

$$W_{EE} = \left[1 + \Delta L_1/L + \Delta L_2/L\right]^{-1} W_{FD} \tag{16}$$

is the corrected dimensionless end effect flowrate. The subscript "*EE*" denotes end effect results. The corrective lengths introduced in the present analysis are provided in Table 1 and includes all results of Table 2 in [28] plus some additional corrective lengths at small values of δ_A always based on the linearized BGK model. The ratio of the simplified fully developed mass flowrate over the corresponding linear and nonlinear ones are given by

$$\frac{\dot{M}_{EE}}{\dot{M}_{LIN}} = \sqrt{\pi}\left(\frac{L}{R} + \frac{2\Delta L}{R}\right)^{-1}\frac{W_{FD}}{W_{LIN}} \tag{17}$$

and

$$\frac{\dot{M}_{EE}}{\dot{M}_{NL}} = \left(1 + \frac{\Delta L_{in}}{L} + \frac{\Delta L_{out}}{L}\right)^{-1}\frac{W_{FD}}{W_{NL}} \tag{18}$$

respectively.

In Table 2, based on Eq. (16), the relative percentage deviation

$$\varepsilon_{EE,LIN} = \left[\left(\dot{M}_{LIN} - \dot{M}_{EE}\right)/\dot{M}_{LIN}\right] \times 100 \tag{19}$$

of the end effect solution (fully developed solution with end effect correction) compared to the linear one, for various L/R and δ_A, is provided. A great improvement compared to the corresponding results obtained by the fully developed solution without end effect correction (shown in Fig. 4), is observed. Now, the end effect results are in excellent agreement with the linear solution for $L/R \geq 10$ across $\delta_A \in \left[10^{-2}, 50\right]$. The discrepancies with the linear solution are increased for $L/R < 10$, particularly at very small values of δ_A, where as it is known the end effect theory becomes less effective [28].

Furthermore, based on Eq. (17) a comparison between end effect and nonlinear results are shown in Figs. 5 and 6. The relative percentage deviation

$$\varepsilon_{EE,NL} = \left[\left(\dot{M}_{NL} - \dot{M}_{EE}\right)/\dot{M}_{NL}\right] \times 100 \tag{20}$$

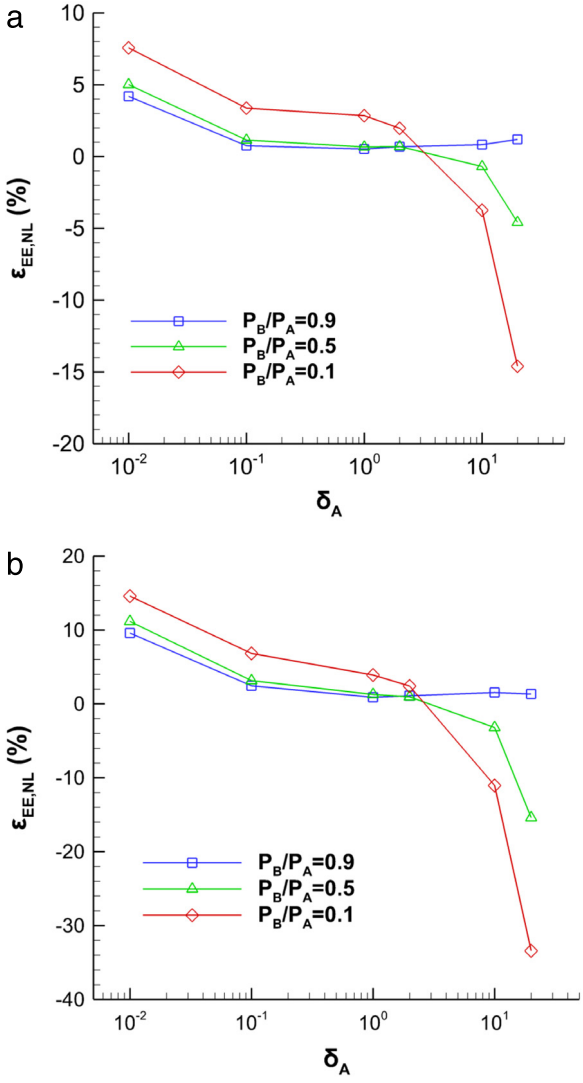

Fig. 5. Relative percentage deviation $\varepsilon_{EE,NL}$ of the end effect solution compared to the nonlinear one in terms of δ_A and various P_B/P_A for flow through tubes of (a) $L/R = 10$ and (b) $L/R = 5$.

is plotted in Fig. 5 in terms of $\delta_A \in \left[10^{-2}, 20\right]$ for $P_B/P_A = [0.9, 0.5, 0.1]$ and $L/R = [5, 10]$. In general, the deviation is relatively small at $\delta_A \in \left[10^{-1}, 10\right]$ and it is increased as δ_A is further either decreased or increased, as well as L/R and P_B/P_A are decreased. A more complete view of the introduced discrepancies is provided in Fig. 6, where $\left|\varepsilon_{EE,NL}\right|$ is plotted in terms of δ_A (L/R) $(1 - P_B/P_A)$. The deviation norm is $\leq$10% for all pressure ratios when $L/R = 20$ and then, for $L/R = 10$ and $L/R = 5$ it remains small when $P_B/P_A \geq 0.1$ and $P_B/P_A \geq 0.9$ respectively.

Based on the results of Table 2 and Figs. 5 and 6 it is concluded that the end effect theory will result to a deviation within ±10% provided that inequality (9) is fulfilled and $L/R \geq 20$. In addition, the deviation norm remains $\leq$10% even for $L/R = 10$ provided that inequality (9) is fulfilled, while $P_B/P_A \geq 0.1$ and $\delta_A \geq 10^{-2}$. This is exactly the great advantage of the end effect correction, since the range of applicability of the infinite capillary theory is

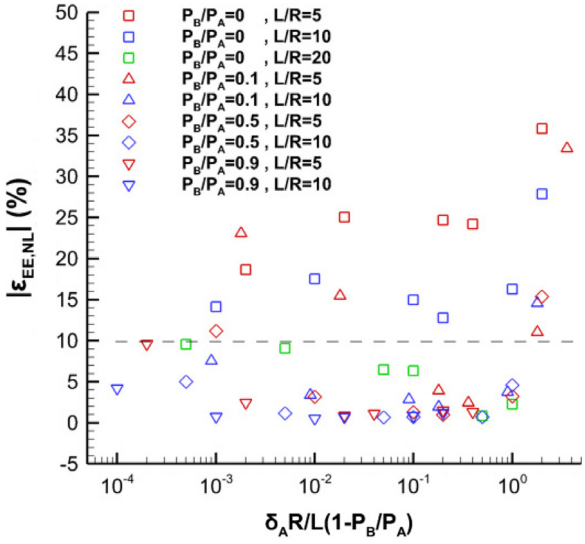

Fig. 6. Norm of the relative percentage deviation $|\varepsilon_{EE,NL}|$ of the end effect solution compared to the nonlinear one for flow through a tube in terms of $\delta_A\,(R/L)\,(1-P_B/P_A)$.

significantly enhanced, while the involved computational effort remains negligible, once the data in Table 1 are available.

4. Concluding remarks

The range of validity of various linear approaches for simulating rarefied pressure driven flow though tubes is computationally investigated. The flowrates obtained by these approaches have been compared to the corresponding nonlinear ones in a systematic manner providing, for an accepted relative deviation norm of $\leq$10%, the specific applicability limits of each linear theory in terms of the input parameters. Overall, the range of validity of the linear solutions is much wider than the expected one, as defined by their mathematical constrains. It is noted that significant savings in computational resources are achieved, when linear (instead of nonlinear) kinetic modeling is introduced.

Acknowledgments

Part of the simulations have performed using the HELIOS supercomputer system at Computational Simulation Centre of International Fusion Energy Research Centre (IFERC-CSC), Aomori, Japan, under the Broader Approach collaboration between Euratom and Japan, implemented by Fusion for Energy and JAEA, as well as "Lomonosov" Supercomputer at Lomonosov Moscow State University.

References

[1] F. Sharipov, V. Seleznev, Data on internal rarefied gas flows, J. Phys. Chem. Ref. Data 27 (3) (1998) 657–706.
[2] L. Mieussens, Discrete-velocity models and numerical schemes for the Boltzmann–BGK equation in plane and axisymmetric geometries, J. Comput. Phys. 162 (2000) 429–466.
[3] F. Sharipov, Numerical simulation of rarefied gas flow through a thin orifice, J. Fluid Mech. 518 (2004) 35–60.
[4] S. Varoutis, Oleg Sazhin, D. Valougeorgis, F. Sharipov, Rarefied gas flow through short tubes into vacuum, J. Vac. Sci. Technol. A 26 (2) (2008) 228–238.
[5] S. Varoutis, D. Valougeorgis, F. Sharipov, Gas flow through tubes of finite length over the whole range of rarefaction for various pressure drop ratios, J. Vac. Sci. Technol. A 27 (6) (2009) 1377–1391.
[6] V.A. Titarev, Efficient deterministic modeling of three-dimensional rarefied gas flows, Commun. Comput. Phys. 12 (2012) 162–192.
[7] S. Misdanitis, S. Pantazis, D. Valougeorgis, Pressure driven rarefied gas flow through a slit and an orifice, Vacuum 86 (11) (2012) 1701–1708.
[8] M.A. Gallis, J.R. Torczynski, Direct simulation Monte Carlo-based expressions for the gas mass flow rate and pressure profile in a microscale tube, Phys. Fluids 24 (2012) 012005.
[9] F. Sharipov, Benchmark problems in rarefied gas dynamics, Vacuum 86 (11) (2012) 1697–1700.
[10] V. Titarev, E. Shakhov, Computational study of a rarefied gas flow through a long circular pipe into vacuum, Vacuum 86 (11) (2012) 1709–1716.
[11] S. Pantazis, S. Naris, C. Tantos, D. Valougeorgis, J. Andre, F. Millet, J.P. Perin, Nonlinear vacuum gas flow through a short tube due to pressure and temperature gradients, Fusion Eng. Des. 88 (2013) 2384–2387.
[12] L. Wu, J.M. Reese, Y. Zhang, Solving the Botzmann equation deterministically by the fast spectral method: application to gas microflows, J. Fluid Mech. 746 (2014) 53–84.
[13] M. Vargas, S. Naris, D. Valougeorgis, S. Pantazis, K. Jousten, Time-dependent rarefied gas flow of single gases and binary gas mixtures into vacuum, Vacuum 109 (2014) 385–396.
[14] G.A. Bird, Molecular Gas Dynamics and the Direct Simulation of Gas Flows, Clarendon, Oxford, 1994.
[15] V.V. Aristov, Direct Methods for Solving the Boltzmann Equation and Study of Nonequilibrium Flows, Springer, 2001.
[16] P.L. Bhatnagar, E.P. Gross, M.A. Krook, A model for collision processes in gases. I. Small amplitude processes in charged and neutral one-component systems, Phys. Rev. 94 (1954) 511–525.
[17] L.H. Holway, New statistical models for kinetic theory: Methods of construction, Phys. Fluids 9 (9) (1966) 1658–1672.
[18] E.M. Shakhov, Generalization of the Krook kinetic relaxation equation, Fluid Dyn. 3 (5) (1968) 95–96.
[19] V.V. Aristov, E.M. Shakhov, V.A. Titarev, S.A. Zabelok, Comparative study for rarefied gas flow into vacuum through a short circular pipe, Vacuum 103 (2014) 5–8.
[20] O.I. Rovenskaya, Comparative analysis of the numerical solution of full Boltzmann and BGK model equations for the Poiseuille flow in a planar microchannel, Comput. & Fluids 81 (2013) 45–56.
[21] T. Fujimoto, M. Usami, Rarefied gas flow through a circular orifice and short tubes, ASME Trans. J. Fluids Eng. 106 (1984) 367–373.
[22] L. Marino, Experiments on rarefied gas flows through tubes, Microfluid. Nanofluid. 6 (2009) 109–119.
[23] S. Varoutis, S. Naris, V. Hauer, C. Day, D. Valougeorgis, Experimental and computational investigation of gas flows through long channels of various cross sections in the whole range of the Knudsen number, J. Vac. Sci. Technol. A 27 (1) (2009) 89–100.
[24] F. Sharipov, Rarefied gas flow through a slit: Influence of the gas-surface interaction, Phys. Fluids 8 (1) (1996) 262–268.
[25] I.A. Graur, A.Ph. Polikarpov, F. Sharipov, Numerical modelling of rarefied gas flow through a slit at arbitrary gas pressure ratio based on the kinetic equation, Z. Angew. Math. Phys. 63 (2012) 503–520.
[26] V.A. Titarev, Rarefied gas flow in a circular pipe of finite length, Vacuum 94 (2013) 92–103.
[27] S. Pantazis, D. Valougeorgis, Rarefied gas flow through a cylindrical tube due to a small pressure difference, Eur. J. Mech. B Fluids 38 (2013) 114–127.
[28] S. Pantazis, D. Valougeorgis, F. Sharipov, End corrections for rarefied gas flows through circular tubes of finite length, Vacuum 101 (2014) 306–312.
[29] F. Sharipov, Rarefied Gas Dynamics, Rarefied Gas Dynamics, in: Fundamentals for Research and Practice, Wiley-VCH, 2016.
[30] S. Pantazis, D. Valougeorgis, Non-linear heat transfer through rarefied gases between coaxial cylindrical surfaces at different temperatures, Eur. J. Mech. B Fluids 29 (2010) 494–509.
[31] V.A. Titarev, Efficient deterministic modelling of three-dimensional rarefied gas flows, Commun. Comput. Phys. 12 (1) (2012) 161–192.
[32] F.M. Sharipov, V.D. Seleznev, Rarefied gas flow through a long tube at any pressure ratio, J. Vac. Sci. Technol. A 12 (5) (1994) 2933–2935.
[33] E.M. Shakhov, Linearized two-dimensional problem of rarefied gas flow in a long channel, Comput. Math. Math. Phys. 39 (7) (1999) 1192–1200.
[34] E.M. Shakhov, Rarefied gas flow in a pipe of finite length, Comput. Math. Math. Phys. 40 (4) (2000) 618–626.
[35] V.A. Titarev, E.M. Shakhov, Efficient method of solution of a problem of rarefied gas flow in a planar channel of large finite length, Comput. Math. Math. Phys. 52 (2) (2012) 269–284.
[36] S. Pantazis, D. Valougeorgis, F. Sharipov, End corrections for rarefied gas flows through capillaries of finite length, Vacuum 97 (2013) 26–29.
[37] D. Valougeorgis, The friction factor of a rarefied gas flow in a circular tube, Phys. Fluids 19 (9) (2007) 091701.
[38] F. Sharipov, I. Graur, General approach to transient flows of rarefied gases through long capillaries, Vacuum 100 (2014) 22–25.
[39] V.A. Titarev, E.M. Shakhov, Rarefied gas flow through a long circular pipe into vacuum, in: 28th International Symposium on Rarefied Gas Dynamics 2012, in: AIP Conf. Proc., vol. 1501, 2012, pp. 465–472.